Cowbot: System Design and Field Evaluation of an Autonomous Weed Mowing Robot for Cow Pastures

Parikshit Maini, Burak M Gonultas, Jim Gaebel, Eric Buchanan,
Minghan Wei, Jack Gust, Pete Kennedy, Pratik Mukherjee and Volkan Isler

I. System Design

In this section, we present Cowbot's system components and discuss the details of its design. We first introduce the base platform used for Cowbot in section I-A and discuss the modifications made to make it suitable for autonomous operations on the pasture. Next, we present operating modes and safety features of Cowbot. We then present the details of the solar-powered charging trailer that is used to charge the Cowbot on the pasture and allows it to be permanently stationed on the farm.

A. The Base Platform

Cowbot is built on the Toro GroundsMaster 3280-D tractor platform which is available commercially and is powered by a 20 kW diesel engine. The platform has a long production history (first launched in 1973) with proven robustness and maneuvering capabilities. It makes for a good choice for the design of Cowbot as it provides sufficient power to operate the mowing implement needed to mow weeds in cow pastures. In line with the focus of the project to reduce carbon footprint in organic dairy production, Cowbot is designed to be powered on the farm using solar power. For this reason, the base platform was modified by replacing the diesel engine with a 100 V high-power 18kW liquid cooled Permanent Magnet AC (PMAC) electric motor powered by a 100V 28.8 kWH lithium battery pack. Cowbot is also equipped with a 6 kW level-2 onboard charger that allows the battery pack to be charged fully in about 6 hours using a level-2 charger. Cowbot is also fitted with the base platform's stock Roll Over Protection System (ROPS) and a canopy strengthened via the addition of front struts. The canopy is also used to provide mounting space for sensors and onboard computer on the Cowbot.

For autonomous control, two key subsystems of the base platform need automation - traction and steering. To achieve automated traction control we replace the manual-input (foot pedal with linkage) hydrostatic transmission control with an electronically-controlled hydrostatic transmission (e-Hydro). The e-Hydro adjusts the transmission swash-plate through electronic control of a forward/reverse coil. The traction subsystem receives speed commands from the traction pedal in manual mode and through navigation commands in autonomous mode. A PID control algorithm that uses speed feedback is used to control the e-Hydro swash-plate to achieve the target speed. Steering on the Cowbot is controlled through a hydraulic cylinder equipped with a position sensor to provide steering feedback. An electronically-controlled solenoid valve is added to provide steer-by-wire functionality. In manual

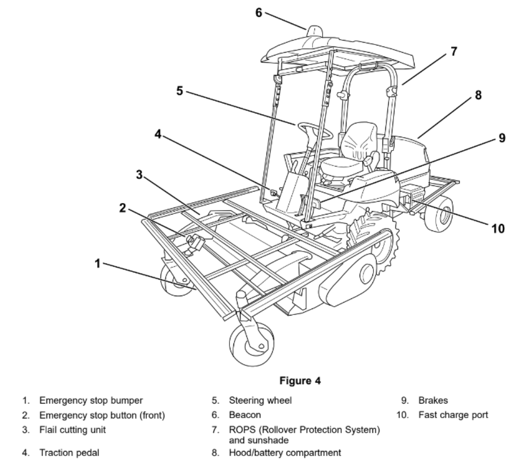

Fig. 1: Annotated image showing different parts of the Cowbot. source: Cowbot manual

mode, the steering wheel pumps oil in and out of the cylinder, while in autonomous mode, the solenoid valve is used to pump the oil in and out of the steering cylinder. The cylinder's stroke length is mapped to centerline steering angle. Autonomous steering commands (in degrees) are converted to a desired cylinder stroke length (analog voltage) using a lookup table. The controller utilizes a proportional control loop to adjust the cylinder stroke to achieve the target steering angle.

When mowing cow pastures to remove weeds, it is desirable to not mow the grass very short to allow it to grow back quickly. Base on recommendations from dairy scientists, we determined a 20 cm height-of-cut (HOC) to be ideal for cow pastures. The common HOC for grass turfs is usually no more than 10 cm. As a result Cowbot's base platform equipped with a rotary cutting implement, was also designed to admit up to 10 cm ($\sim$ 4") HOC. During initial tests, rotary mowers were found unacceptable due to the inability to achieve the large HOC, high power consumption in pasture conditions and the risk of flying debris thrown at high speeds. For this reason, the Cowbot was equipped with a flail cutting implement with 60 inch ($\sim$ 152 cm) wide deck custom mounted to provide 20 cm HOC. Incorporating the flail is a challenging task, because the added vertical translation of this taller, close-mounted attachment (as compared to rotary cutting implement) creates a very tight fit under the platform with limited ground clearance. Further, the low-profile of the tractor provided minimal ground clearance for the flail to follow the terrain. As a result, the entire tractor body was raised (via axle spacers) to allow additional clearance for the front mounted flail over undulating terrain. The standard turf-tread traction drive tires were also replaced with tractor-lug tires to provide extra traction and ground clearance.

Since, the flail cutting implement throws the grass towards the back as against a rotary implement that throws to the side, a shield was added behind the flail deck to prevent debris from wrapping around the 4WD driveshaft. Under-body transmission oil filters are re-positioned and guards were added due to minimal ground clearance. A quick-attach design was created to simplify flail installation. Additionally, a front-end hitch system was created to allow the tractor to "pull" a field cultivator by going in the reverse direction, Cowbot design and mechanical modifications ensure satisfactory performance and robustness in the field. It has sufficient power, energy, maneuverability, and traction to complete its objectives on the rough and challenging terrain on cow pastures. A drawback to Cowbot's design identified during large-scale field experiments is that the compact wheelbase and tall profile can create high degrees of pitch and roll over the rough terrain.

B. Autonomous Operation

Cowbot can operate in both manual and autonomous modes. In the manual mode, it is controlled by the traction pedal and steering wheel. In the autonomous mode, it receives steering and traction commands through CAN messages from the onboard computer. In this subsection, we present the details of these two modes and the switching protocol between them.

For safety considerations, Cowbot's autonomous mode is designed to be initiated by a human (operator). This is achieved by a manual to autonomous mode hand-off protocol. Cowbot has 4 operating states/modes: Manual, Arm, Ready and Auto. When autonomous operation is desired, the operator sets the Cowbot to Arm mode by pressing the arm button on the console. In Arm mode, the electronic steering system is activated, Cowbot states are recorded, the three onboard (wired) E-stops and the wireless E-Stop need to be enabled (to make sure the machine can be stopped any time for safety). Once the Cowbot is ready, the operator initiates the transition to Ready state by pressing the Arm button again. Ready state is solely a transition state and means the Cowbot is ready to operate autonomously. Cowbot will stay idle in this state waiting for the onboard computer to send a mode command for Auto mode. On receiving the Auto in the mode command from the computer, Cowbot transitions to Auto mode. The operating mode of Cowbot and the computer are sent as identical messages on the CAN bus. Both systems must indicate that their mode is Auto or the Cowbot will revert to Manual mode. If either system stops sending the message, a bus timeout error will cause the Cowbot to revert to Manual mode.

Cowbot uses a GPS-based point to point inertial navigation system and is equipped with two multi-band RTK GNSS receiver units (SwiftNav Duro Inertial) with inbuilt IMU sensors to provide high accuracy location and heading estimates. It is also equipped with front facing imaging sensors that includes two RGB-D cameras (Intel RealSense D455) and a lidar sensor (Velodyne Puck VLP-16). The perception stack of the Cowbot that aims to build capability for visual inertial navigation and weed detection on the field is currently under development. The sensors connect to an onboard computer (Dell Precision 7530) that runs the navigation software. The navigation software on Cowbot has a three-layer architecture. The top and middle layers execute on the computer and the bottom layer executes on a programmable logic controller (TORO PLC model # - Tec 5004) that controls the traction and steering systems discussed in Section I-A. The top layer is the perception and planning layer that takes input from the user and on-board sensors, and plans paths for the mower. The middle layer comprises of high level control modules for point to point navigation. It communicates with the top layer over the Robot Operating System (ROS) and takes as input the waypoint path computed by the planner. It generates steering and speed commands for the bottom layer. The middle and bottom layers communicate using CANBUS messaging protocol. When in the Auto mode, the navigation command is sent from the onboard computer via CANBUS. The command must be sent at a periodic rate so that a message timeout can be detected which would cause Autonomous operation to cease and switch into the manual mode. The Navigation Command includes desired traction speed, desired steering angle, desired motor operation speed (discrete levels) and operation commands including lift or lower for the cutting implement and PTO to turn the cutting implement on. The CANBUS interface allows full operational control of the Cowbot while relying on the electrical subsystem discussed in Section I-A for the low level control of the Cowbot's components.

C. Safety Systems

Cowbot is designed to autonomously operate large weeding implements in challenging terrain on cow pastures. Safety of operation is of primary concern in its development and a variety of operational safety systems have been implemented in the design.

- Operational Procedure: Unlike many existing agricultural robotic platforms, Cowbot qualifies as heavy machinery due to its size and power. Additionally, the intended operational environment in dairy farms is shared with livestock and human workers. In the current stage of development and agricultural autonomy, we think it is essential for a human operator to be aware that a large autonomous robot is operating on the pasture. To enforce this, we require that an operator initiates Cowbot's transition to Autonomous operating mode. As detailed in section I-B, the operator must go through a multi-step state transition process to enable Autonomous mode on the Cowbot.
- Bump Sensors: Cowbot is surrounded with force-activated bump sensors on all sides. In the event that the Cowbot runs into an obstacle, the bump sensor will activate and signal the motor controller to stop the motor. This will cause all hydraulics to deactivate and completely stop the machine.
- Flail Guard: As mentioned earlier, Cowbot is equipped with a flail-deck cutting implement to cut weeds. Further,

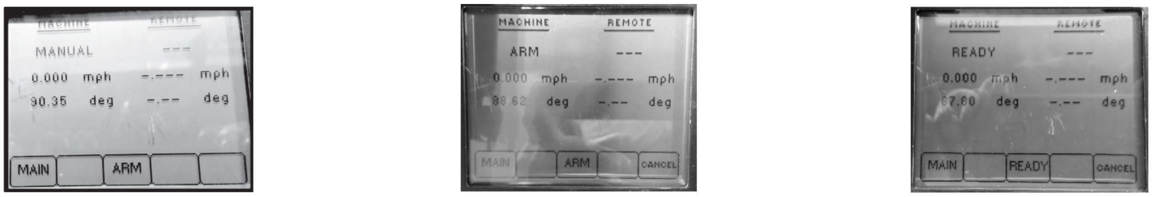

(a) Manual mode (b) Arm mode (c) Ready mode

Fig. 2: Operator console view showing different operating modes of the Cowbot.

the flail implement is custom mounted to achieve a 20 cm height of cut. In case of the standard mount position of the flail-deck at around 10 cm height of cut, the ground clearance is sufficiently low to prevent objects on the ground to be thrown to the front by the spinning flail blades. However, in the case of Cowbot, a flail guard is deployed in the front of the deck by making a curtain of heavy chains that obstruct any objects picked up by the spinning blades to be thrown to the front.

- Flashing Lights: When operating in Autonomous mode, a bright flashing beacon light mounted on top of the Cowbot turns on to attract attention and give a clear warning sign to the viewer.
- Wired E-Stop Switches: There are three wired one-press E-Stop switches on the Cowbot mounted in the front, back and on the operator console on the right side of the Cowbot. To initiate Auto mode, all E-stops must be active. In the event of unintended operation, an emergency stop can be initiated by a human (operator) by pressing and engaging any of the three E-stop switches. On pressing an E-stop switch, Cowbot will be powered off and the motor will stop operating to completely disable its operations. Each of the E-stop switches must be disengaged to power on the Cowbot again.
- Wireless E-Stop Switch: A one-press wireless E-Stop switch is also provided with the Cowbot to allow a human (operator) to stop it remotely when in Autonomous mode. It communicates with the Cowbot on the 2.4 Ghz band. The Cowbot will transition to autonomous mode only if the wireless E-Stop is turned on and remote connection is established. When the wireless E-Stop switch is engaged, Cowbot's controller will turn off the motor and exit Autonomous mode. This implementation is intended to ensure that the Cowbot can be safely and reliably disengaged when needed. In the case that the wireless E-Stop goes out of range of the Cowbot when it is operating in Autonomous mode, Cowbot will failsafe - the controller will turn off the motor and exit Autonomous mode. The wireless E-Stop must be disengaged before the Cowbot can be powered on again.
- Failsafe to manual: Potential usecase for Cowbot includes a human operator sitting on the tractor but operating in autonomous mode. In this case, to allow easy control of Cowbot in case of undesired behavior in Auto mode, any input on the traction pedal or steering wheel triggers failsafe behavior and transitions the Cowbot state to Manual. The Cowbot seat is also connected to a switch and an operator can be in or out of the seat, but a change of state in Auto mode triggers the switch and transitions the Cowbot state to Manual.

D. Solar Charging Trailer

Weed removal on large dairy farms requires sustained operations over multiple days and availability of recharging infrastructure on the farm to recharge the Cowbot. For this reason, we designed a solar-powered charging trailer to recharge Cowbot's batteries and allow it to be stationed on a farm over multiple days. In this subsection, we present the design of the charging trailer that allows off-the-grid charging for Cowbot. It is designed to fully enclose the Cowbot and is also used to transport the Cowbot over large distances between remote pastures. The solar-powered trailer can be deployed on the pasture and provides a level-2 charging terminal to charge Cowbot's batteries. Fig. 3 shows the outside and inside views of the charging trailer. The trailer is a tandem axle, V-nose trailer (Stealth Enterprises) and measures 4.3 m x 2.1 m. Cowbot's canopy was redesigned to fold-back to allow entrance into the enclosed solar charging trailer for transport.

An important prerequisite to design an off-grid solar-powered charging system is to determine the power and energy requirements of the electrical load and how long the energy storage system must supply that load without sunlight. In our application, load is the autonomous mower's battery pack that comprises $\sim$29 kWh of energy when fully charged. Ideally, the trailer and mower batteries would be recharged daily. Based on the average solar insolation in central Minnesota during the summer months (4.5-4.9 kWh/m^2/day [1]), a solar array of about 3.1 kW is required to meet the daily load (source, reference). We use ten solar panel modules (GCL-6P/72) of 325 Watt power rating to provide a 3.25 kW array needed to satisfy the load requirement. Each panel measures 1956 × 992 × 35 mm in size and weighs 22.2 kg. Area on the roof of the trailer can only fit four panels. For this reason, we opted for a design with retracting brackets that extend over the sides of the trailer to mount the panels. The mounting bracket is designed and attached to the trailer roof to hold four fixed panels. Under the fixed panels, there are two lower rows of three panels each that are mounted on fully extending, heavy-duty, drawer slides. It allows each row to slide out to access sunlight, one to the left side of the trailer and the other to the right side. When in transportation, the two rows are retracted under the fixed panels.

To design the trailer battery system we considered multiple factors including the degree of discharge (DoD) on trailer

(a) Solar-charging trailer (b) Trailer Electricals

Fig. 3: The inside and outside view of the solar panel trailer.

and mower batteries, trailer towing weight and budgetary restrictions. There is an inverse relationship between DoD and battery life: allowing batteries to discharge more, reduces the number of charge/discharge cycles of the battery. A DoD of 35% was selected as a reasonable compromise between mowing capacity, battery life and reserve capacity, leading to a daily recharging load for the trailer battery pack of 18.9 kWh based on practical experiments. We use eight 6v 375 Ah deep-cycle lead acid batteries (model: Trojan SAGM 06 375 solar batteries) connected in series to make a 48 volt battery pack with a combined storage capacity of 18.3 kWh. Each battery weighs 52 kg resulting in a total battery pack weight of 416 kg.

The panels are wired as five parallel pairs of two panels each in series. Paired wiring connections lessen the overall impact of shading on individual panels and keeps the resultant voltage and current within the input specifications of the charge controller that manages the battery charging process. The solar panel output wires are fused in a combiner box which feeds directly into an 80 Amp charge controller (AIMS SCC80AMPPT). DC output from the battery pack is wired to a 6 kW power inverter (AIMS PICOGLF60W48V240VS) which converts it to AC and feeds the load center to be distributed to any AC loads. The AC loads comprise 120V outlets and a 240V Level 2 electric vehicle charger (Clipper Creek LCS-30-C12-L25-53) that provides a 24 Amp/5.8 kWh charging terminal via a J1772 connector.

II. Planning and Control

A. Coverage Path Planning

To mow weeds on the pasture we compute coverage paths for the Cowbot. A path planner for the Cowbot must ensure that the entire pasture is covered and the path length is minimized. However, there are additional considerations when operating on challenging terrain in cow pastures. In the presence of hills and slopes on the pasture, it is safer to drive up and down the slope rather than across the slope due to the risk of toppling of the vehicle. Further, the space needed to turn around the vehicle near the boundary of the pasture, also called headland or turn areas, can create challenges to ensure coverage and adds overhead to the length of the path. For this reason, we present multiple path planners that may be used in different environments and conditions.

1) Adjacent Row Path Planner: Paths computed by adjacent row path planner comprise of adjacent to-and-fro passes across the length of the field in alternating directions. The width of each pass is equal to the width of the mowing implement on the mower. This path pattern is also known as boustrophedon or lawn mower pattern. It is the most common pattern used in mechanical mowing as it allows an operator to mow straight lines by following the contour of the previous pass. Since consecutive passes are adjacent to each other, the mower must make a sharp turn at the end of each pass to move to the next pass. As the turn diameter of Cowbot is larger than the distance to the next pass (width of the cutting implement), additional space (headland) is needed at the two ends of the field for the Cowbot to turn around and move to the next pass. This is a very common scenario with farm vehicles and there exists a body of literature [2] that focuses on minimizing the width of the headland using various turning maneuvers like fishtail and lightbulb (also called omega) turns. In our implementation we use light-bulb turns at the end of each pass to move to the next pass.

2) Skip-Row Path Planner: Similar to the adjacent-row planner, the skip-row planner also comprises of to-and-fro passes across the length of the field in alternating directions. However, unlike the adjacent-row planner, it does not require consecutive passes to be adjacent and allows the Cowbot to skip rows between consecutive to-and-fro passes on the coverage path. It plans paths for the Cowbot such that the distance between consecutive passes is more than the turn diameter. This allows the Cowbot to turn around to move the next pass without needing additional space at the end of the pass. Our implementation of the skip row planner admits multiple rows between passes allowing 90° sharp turns and reduces the width of the required headland to the minimum space needed for the Cowbot to traverse (equal to the width of the cutting implement). Even though the skip-row planner reduces the width of the headland at both ends, the length of the path traversed when moving between passes adds to the overhead as it repeatedly mows on the same area and does not contribute to coverage.

3) Spiral Path Planner: The spiral path planner computes a path for the Cowbot that starts along the boundary of the pasture and gradually moves inward in a spiral pattern. The path starts by following the perimeter of the pasture. At the end of a round of the spiral path, the planner shrinks the size of the pasture along each edge to remove the covered area from consideration. To compute the new perimeter, each edge of the pasture is moved inward by distance equal to the width of the cutting implement. Subsequent round of the spiral path follows the new perimeter that encloses the uncovered area. The spiral planner terminates when the uncovered area on the pasture shrinks to zero. A spiral path does not revisit any location on the pasture. It removes the need for headlands and does not add any overhead on path length. This allows the spiral planner to be most efficient in terms of total path length amongst the three planners. However, in the case of slopes and hills on the cow pasture, path computed by the spiral planner may not be feasible for the Cowbot. This is because traversing across slopes is not recommended for larger farm vehicles like Cowbot as it can lead to toppling of the vehicle. Spiral planner requires the Cowbot to traverse in all directions over the course of the planned path and hence is not well-suited for slopes.

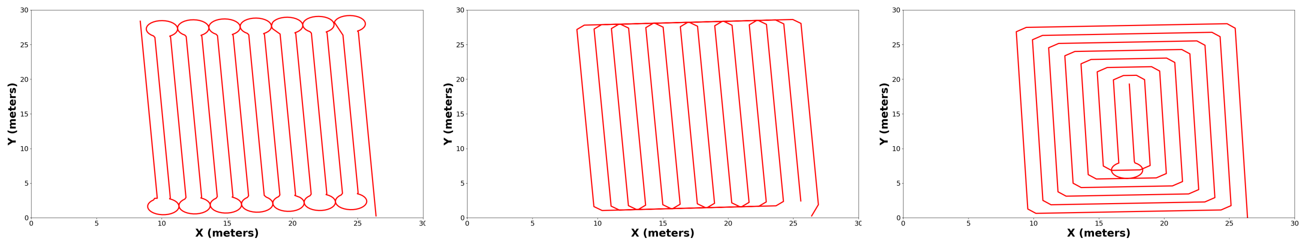

(a) (b) (c)

Fig. 4: Figures show sample paths planned by the three planners: (a) adjacent-row path planner (b) skip-row path planner (c) spiral path planner

4) A note on irregularly shaped pasture coverage: Cow pastures can comprise large tracts of land and have different local features even within the same pasture. In our field evaluations we found that dividing a pasture into smaller fields by topography allows the use of the most-suitable planner for each field. There are a number of cellular decomposition methods in the literature that may also be used for dividing a pasture into smaller fields. We refer the interested reader to those papers for details on such methods. We restrict our division of the pasture to convex polygon shaped fields. The use of adjacent-row and skip-row planners in a convex polygon shaped field is straight-forward. Identify the longest edge of the field and plan all passes on the path to be parallel to it. The length of each pass is determined by the intersection of the pass with the two edges of the field on either side minus the width of the headland at each end. The spiral planner does not require any modification. It starts by following the perimeter of the field. At the end of the first round of the spiral path, it computes a new perimeter of the field that comprises only the uncovered area by moving all edges towards the interior of the field by distance equal to the width of the cutting implement. The path then follows the new perimeter to compute the next round of the spiral. The planner iterates this process to compute subsequent rounds of the spiral path and terminates when the uncovered area of the field shrinks to zero.

B. Kinematic Model

In this section we develop a geometric model for Cowbot's kinematics. Cowbot is built on a four-wheeled rear steered platform with traction on the front two wheels. To design a navigation controller for the Cowbot, we need to model its kinematics. In previous work, Rajamani [3] designed a geometric model for vehicles with independent steering control on both front and rear wheels, and described its extension to front steered vehicles. Since a rear steered vehicle turns opposite to the steering angle direction, there are important differences from Rajamani's vehicle model. We extend their model to rear steered front wheel drivetrain vehicles and derive the associated kinematic equations. We use a bicycle model to represent the four wheeled robot (similar to [4] and [3]) where the front two wheels and the rear two wheels are each represented by a single wheel at the front and rear of the bicycle model, respectively. The robot is assumed to operate in the two dimensional plane with zero slip at either of the two wheels. The zero slip assumption is standard in the literature [3] and holds true at low speeds.

Consider the top view of the bicycle model shown in Figure 5. The front wheel of the model is centered at $\mathcal{F}$ and the rear wheel is centered at $\mathcal{B}$. Wheel base of the bicycle model is of length L. The robot moves with a speed v with heading angle θ about the positive x-axis. The velocity at each of the wheels is in the direction of motion of the wheels and is shown in the figure with dashed arrows. Steering angle of the rear wheel, δ, is measured with respect to the longitudinal axis of the robot model. Both, heading and steering angles of the model are measured in the counter clockwise direction. As shown in the figure, the robot turns in the direction opposite to the steering angle of the rear wheel. This is because the instantaneous center of rotation (ICR), found as the intersection of the rotation axes of the front and rear wheels, is located on the opposite side at $\mathcal{I}$ resulting in an angular velocity in the direction opposite to the rear wheel steering angle.

We consider a 3-tuple state for the bicycle model, $< x, y, \theta >$. Here (x, y) are the location coordinates of a fixed reference point on the model and θ is the heading direction of the bicycle. The inputs to the model are the magnitude of the velocity, v, and the steering angle of the rear wheel, δ. The choice of reference point may be driven by the application. For instance, in the case when a sensor or actuator is mounted in the front of the robot, the center of the front wheel of the bicycle would be an obvious choice for the reference point. Other applications might require the rear end or another point on the robot to be tracked as the reference point. In the following, we consider three reference point locations on the model and derive the kinematic equations for the bicycle model at each of these points.

1) Reference point at the center of gravity: Consider the bicycle model geometry in Figure 5 that shows the reference point location at the center of gravity of the bicycle model. Let the coordinates of the reference point be $\mathcal{C} \equiv (x_c, y_c)$. On the four wheeled robot, this point corresponds to the center of gravity on the longitudinal axis of the robot. The direction of motion at $\mathcal{B}$ is at an angle $\boldsymbol{\beta}$ with respect to the longitudinal axis. $\boldsymbol{\beta}$ is called the slip angle. To derive the state gradient equations for the bicycle model, we consider $\triangle\mathcal{FIC}$ and $\triangle\mathcal{FIB}$. The slip angle $\boldsymbol{\beta}$ at the reference point $\mathcal{C}$ can be

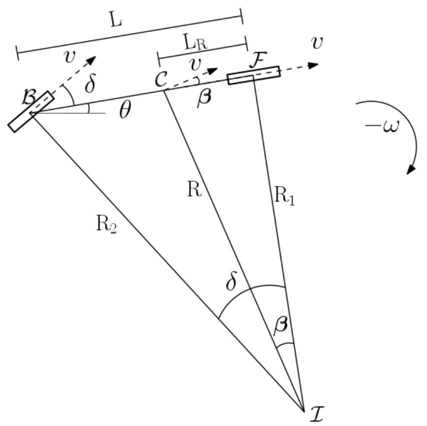

Fig. 5: Bicycle model for a rear steered vehicle with front wheel drivetrain. The figure shows the steering geometry when the reference point is located at the center of gravity of the robot ($\mathcal{C}$).

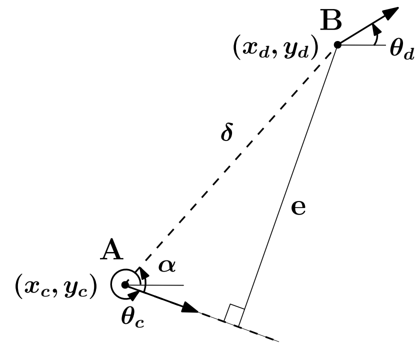

Fig. 6: Engagement geometry for Cowbot's geometric path following controller.

calculate as follows:

$$\tan\delta = \frac{\mathrm{L}}{\mathrm{R_1}} \quad \Rightarrow \quad \mathrm{R_1} = \frac{\mathrm{L}}{\tan\delta} \tag{1}$$

$$\tan\boldsymbol{\beta} = \frac{\mathrm{L_R}}{\mathrm{R_1}} \quad \Rightarrow \quad \mathrm{R_1} = \frac{\mathrm{L_R}}{\tan\boldsymbol{\beta}} \tag{2}$$

Using equations (1) and (2),

$$\frac{\mathrm{L}}{\tan\delta} = \frac{\mathrm{L_R}}{\tan\boldsymbol{\beta}} \quad \Rightarrow \quad \boldsymbol{\beta} = \arctan\left(\frac{\mathrm{L_R}}{\mathrm{L}}\tan\delta\right) \tag{3}$$

The turn radius R at the reference point $\mathcal{C}$ may be calculate using equation (1) as follows:

$$\cos\boldsymbol{\beta} = \frac{\mathrm{R_1}}{\mathrm{R}} \quad \Rightarrow \quad \mathrm{R} = \frac{\mathrm{R_1}}{\cos\boldsymbol{\beta}} = \frac{\mathrm{L}}{\tan\delta\cos\boldsymbol{\beta}} \tag{4}$$

We can now write the equations for the state gradient as follows:

$$\dot{x} = v\cos(\theta + \boldsymbol{\beta}) \tag{5}$$

$$\dot{y} = v\sin(\theta + \boldsymbol{\beta}) \tag{6}$$

$$\dot{\theta} = -\omega = -\frac{v}{\mathrm{R}} \;=\; -\frac{v}{\mathrm{L}}\tan\delta\cos\boldsymbol{\beta} \tag{7}$$

C. Navigation Controller Design

In this section, we present the design of the lateral control law deployed on the Cowbot for path-following. Cowbot uses a geometric path-following controller for steering control. We refer to the controller as *Cowbot* control law. The Cowbot control law is suitable for tracking curved paths and provides global convergence to the reference trajectory from any starting location. It combines the requirements to align robot heading with desired heading, eliminate cross-track error and keep the steering angle within the maximum steering limits.

We show the engagement geometry for a wheeled mobile robot with a finite turning radius tracking a reference point in figure 6. The robot is represented using a point mass located at its geometric center. The figure shows the robot's current location, $A \equiv (x_c, y_c)$, and heading angle, θ_c. The desired location and heading angle on the reference trajectory for the robot are shown as $B \equiv (x_d, y_d)$ and θ_d respectively. We define the heading error, $\phi \in [-\pi, \pi]$, as the angular difference between the current heading and the desired heading with respect to the current heading. The cross-track error, $\mathbf{e} \in \mathbb{R}^+$, is the shortest distance to the desired location from the direction of travel of the robot. We also define LOS (Line-of-Sight) distance, $\delta \in \mathbb{R}^+$, as the euclidean distance between robot's current and desired locations and LOS angle, $\alpha \in [-\pi, \pi]$, as the angle that the LOS line (**AB**) makes with the robot's heading direction. We note from Figure 6 that

$$\sin\alpha = \frac{\mathbf{e}}{\delta} \tag{8}$$

The Cowbot lateral controller steers the robot to drive both cross-track error and heading error to zero. The steering angle, ω, is assumed to lie in the range $[\omega^-, \omega^+]$, where ω^- and ω^+ are the minimum and maximum steering angles of the robot, respectively. The control law is expressed as:

$$\omega = k_p\alpha + k_h\frac{\phi}{\max(c, \delta)} \tag{9}$$

where, c is a small finite constant, k_p is the proportional gain and k_h is the heading gain. The Cowbot control law has two components. The first component is a proportional controller that steers the robot to bring the LOS angle to zero. It directly affects the cross-track error. The second component is proportional to the heading error and inversely proportional to the LOS distance. When the robot is farther away from the reference point, the inverse proportionality to LOS distance makes the first component of the control law dominant. As the robot nears the desired location, the second component ensures that the robot heading is aligned with the desired heading angle. c ensures a finite value in the denominator of the second component. We fix the value of c to be equal to the distance tolerance. Thus, when $\delta == c$, the desired location is moved to the next point on the reference trajectory. Value for k_p and k_h are determined experimentally.

$$\omega = k_p\sin^{-1}\frac{\mathbf{e}}{\delta} + k_h\frac{\phi}{\max(c, \frac{\mathbf{e}}{\sin\alpha})} \tag{10}$$

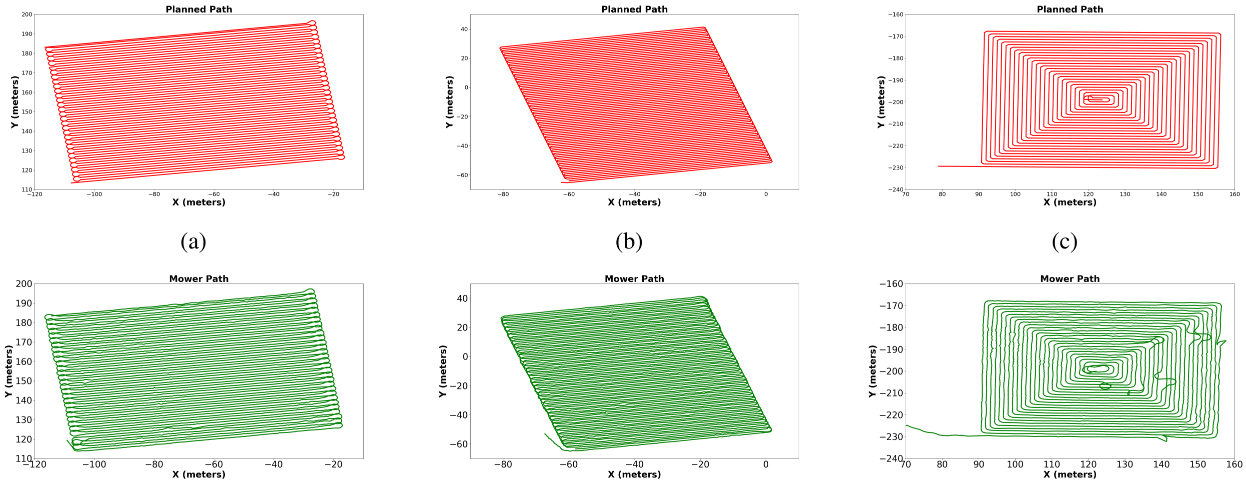

(a) (b) (c)

(d) (e) (f)

Fig. 7: Figures show paths planned by the three planners and the actual paths followed by Cowbot. Adjacent-Row Path Planner: (a) planned (d) actual; Skip-Row Path Planner: (b) planned (e) actual; Spiral Path Planner: (c) planned (f) actual

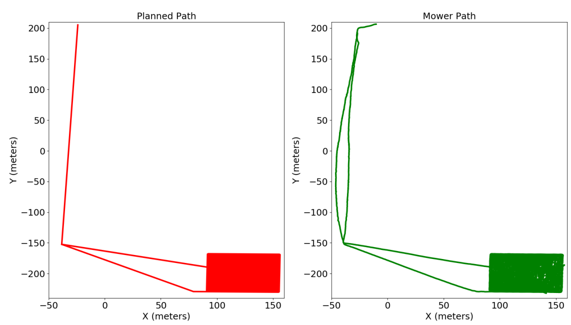

Fig. 8: Spiral path showing the return to home functionality of the Planner.

III. Field Evaluation

Cowbot was tested through an extensive field evaluation procedure covering 6 adjacent 1-acre cow pastures in Morris, Minnesota. During the field experiments, all 3 coverage path planning algorithms discussed in II-A were tested in separate 1-acre pastures. Remaining 3 pastures were mowed by a human operated pasture mower as the baselines. The test pastures presented a rugged environment to Cowbot as well as dense and large weed populations. The navigation controller presented in II-C was developed and tuned to make the Cowbot safely and successfully navigate in environments with varying topography including grasslands, cow pastures, hills, valleys with dense weed populations and rough terrain. In addition to large scale field experiments in 1-acre cow pastures, Cowbot was also tested at night. Cowbot was able to complete its operation successfully and mow the designated area without human intervention at night. Night experiments have demonstrated that the proposed autonomous weed control platform is able to operate without daylight, using GPS signal for its navigation system.

Planner Name	SoC at Start	SoC at End
Adjacent Row Path Planner	93	39
Skip Row Path Planner	96	37
Spiral Path Planner	71	36

TABLE I: State of Charge (SoC) for each experiment run showing the total energy consumed in percentage.

Field evaluations show that Cowbot is a suitable platform for mowing weeds on pastures with difficult to navigate rough terrain and our presented coverage path planners working together with our control algorithms are well suited for the task in terms of operational and computational efficiency on real-time systems.

References

[1] M. Sengupta, Y. Xie, A. Lopez, A. Habte, G. Maclaurin, and J. Shelby, "The national solar radiation data base (nsrdb)," *Renewable and Sustainable Energy Reviews*, vol. 89, pp. 51–60, 2018. [Online]. Available: https://www.sciencedirect.com/science/article/pii/S136403211830087X

[2] D. Sabelhaus, F. Röben, L. P. Meyer zu Helligen, and P. Schulze Lammers, "Using continuous-curvature paths to generate feasible headland turn manoeuvres," *Biosystems Engineering*, vol. 116, no. 4, pp. 399–409, 2013. [Online]. Available: https://www.sciencedirect.com/science/article/pii/S1537511013001414

[3] R. Rajamani, *Vehicle dynamics and control*. Springer Science & Business Media, 2011.

[4] D. Wang and F. Qi, "Trajectory planning for a four-wheel-steering vehicle," in *Proceedings 2001 ICRA. IEEE International Conference on Robotics and Automation (Cat. No. 01CH37164)*, vol. 4. IEEE, 2001, pp. 3320–3325.